RSC Advances

PAPER

View Article Online
View Journal | View Issue

Cite this: *RSC Adv.*, 2025, **15**, 42347

Cyclodextrin-threaded covalent organic polyrotaxanes with tunable solid-state emissive activity for efficient iodine capture

Xia Guo,[a] Xueling Zhou,[a] Qiupeng Gu,[a] Xiaohong Zhang[a] and Yanyan Tang *[b]

Herein, we rationally designed and synthesized a covalent organic polyrotaxane (COPR), with aggregation-induced emission (AIE) characteristics, denoted as TPE-CD-COPR, through a two-component Knoevenagel condensation reaction, where β-cyclodextrin (β-CD) inclusion complexes served as direct building blocks. This approach yielded several remarkable improvements over conventional CD-free counterpart (TPE-COP). The threading of CD not only achieved precise tuning of solid-state emission color under UV irradiation, but also introduced significant polarity enhancement through rotaxane subunit incorporation. The incorporation of water-soluble cyclodextrin rotaxane architectures significantly enhanced the aqueous dispersibility, thereby providing an optimal solution for developing high-performance aqueous-phase iodine adsorbents. As a result, TPE-CD-COPR demonstrated significantly enhanced aqueous-phase iodine adsorption capabilities, exhibiting both superior capacity and faster kinetics compared to conventional CD-free counterpart. The enhanced I_2 adsorption capacity arises from synergistic effects of hydroxyl-rich β-CD threading, multiple oxygen coordination sites, π-electron rich fully conjugated framework, and the complementary nitrogen/cyano adsorption sites. Meanwhile, TPE-CD-COPR also showed excellent recyclability (99% capacity retention after 5 cycles). This groundbreaking synthetic strategy establishes a versatile platform for constructing polyrotaxane-based porous organic polymers (POPs) with tailored photophysical properties, and multifunctional adsorption capabilities, significantly expanding the application potential of porous materials in environmental remediation.

Received 17th August 2025
Accepted 20th October 2025

DOI: 10.1039/d5ra06071k

rsc.li/rsc-advances

Introduction

Covalent organic polymers (COPs) have emerged as a revolutionary class of artificial porous materials over the past decade, garnering significant attention in materials science.[1] Their most distinctive advantage lies in the precisely programmable architecture and tailorable functionality, enabling rational design for targeted applications through molecular-level engineering.[2] To date, researchers have developed thousands of structurally diverse COP variants with tunable pore sizes and surface areas, finding applications spanning from advanced photonics to cutting-edge biomedical technologies.[3–5] Particularly noteworthy is the challenge of polarity modulation, a critical yet elusive parameter that fundamentally governs the key material property of the adsorption capacity (polarity-dependent host–guest interactions).[6] Despite extensive research efforts, precise polarity control remains one of the most formidable challenges in COP development due to complex interplay between building block chemistry and supramolecular organization, difficulties in maintaining porosity while introducing polar groups, and lack of standardized characterization methods for surface polarity.[7–9]

The development of porous polymers with tailored polarity faces significant hurdles due to inherent limitations in conventional synthetic approaches. The traditional bottom-up approach is hampered by escalating inefficiencies, because its convoluted synthetic routes drain time and resources while yielding ever smaller returns.[10] Top-down strategies promise theoretical advantages yet grapple with their own obstacles, as steric and electronic constraints routinely limit functional group conversions to less than sixty percent and the lack of precise spatial control produces an inconsistent mixture of products.[11] These interconnected limitations create a perfect storm of challenges. Therefore, for the rapid development and real applications of COPs, novel materials with concurrently economical and straightforward manufacturing, as well as adjustable physical characteristics are urgently needed.[12]

Iodine (I_2) is a common water pollutant originating from nuclear waste discharge, medical disinfectants, and industrial processes.[13] Due to its high mobility in aqueous environments and potential toxicity, effective removal is crucial for environmental and public health safety.[14] Physical adsorption remains the most widely used method for iodine capture due to its simplicity, scalability, and cost-effectiveness.[15] This process

[a]*School of Mathematics and Statistics, Weifang University, Weifang, Shandong, PR China. E-mail: 736308663@qq.com*
[b]*School of School of Physics and Electronic Infor, Weifang University, Weifang, Shandong, PR China*

relies on multiple interaction sites to enhance iodine uptake, including the porous structures, electron-rich functional groups (heteroatom sites), and π-conjugated systems.[16] Despite its popularity, designing materials with optimal adsorption sites remains a major research challenge.

Cyclodextrins (CDs), a class of cyclic oligosaccharides linked by α-1,4-glycosidic bonds, have emerged as versatile building blocks in materials science due to their unique structural and physicochemical properties.[17,18] One of the most distinctive structural features of CDs is their conical hollow cylinder architecture, which combines a hydrophobic inner cavity with a hydrophilic outer surface. This unique three-dimensional (3D) toroidal structure enables the formation of stable inclusion complexes with various hydrophobic drugs and aromatic compounds.[19] Cyclodextrin-based covalent organic polymers (COPs) have emerged as a research frontier in environmental science and biomedical engineering.[20,21] However, current studies predominantly focus on direct utilization of native CDs or their derivatives as building blocks, which has limited the diversity of accessible polymeric structures. To date, only a limited number of CD-based polymers have been successfully synthesized. Notably, CDs and their derivatives occupy a central position in supramolecular chemistry, where they are widely employed as key components for constructing mechanically interlocked molecules through noncovalent self-assembly strategies. Their exceptional host-guest recognition properties make them indispensable tools in the bottom-up fabrication of complex supramolecular architectures.[22] This structural versatility, combined with their biocompatibility, positions CDs as ideal molecular platforms for developing advanced functional materials with tailored properties for specialized applications.

Here, we employed a supramolecular chemistry approach to fabricate COPs, successfully synthesizing covalent organic polyrotaxanes (COPRs) through the threading of aldehyde-functionalized aromatic organic blocks with β-cyclodextrin (β-CD). The incorporation of high-molecular-weight β-CD (M_w = 1135) into the porous framework significantly reduced material costs, under identical molar amounts of monomers, TPE-CD-COPR exhibited a 3.12-fold increase in weight compared to non-rotaxanated COP under similar reaction units. Moreover, the oxygen-rich structure of β-CD enhanced the polarity of polymer skeleton, as evidenced by substantially improved iodine (I_2) uptake capacity. Notably, the solid-state aggregation-induced emission (AIE) properties could be precisely modulated *via* the CD-threading strategy. Our findings highlight that integrating supramolecular chemistry into porous polymer networks offers a straightforward and efficient strategy for designing high-performance solid-state photoluminescent emitters with tunable emission color and intensity. Furthermore, the threading of CD into polymer skeletons provides a facile method for regulating otherwise challenging-to-control physical properties, accelerating R&D processes and expanding potential applications. This work underscores the versatility of supramolecular approaches in tailoring advanced functional materials for diverse technological applications.

Results and discussion

The synthetic routes for both cyanostilbene (CS) based COPs follow previously reported protocols (Scheme 1).[23] Aldehyde-functionalized monomers, including the 1,4-phthalaldehyde and its cyclodextrin inclusion complex, underwent

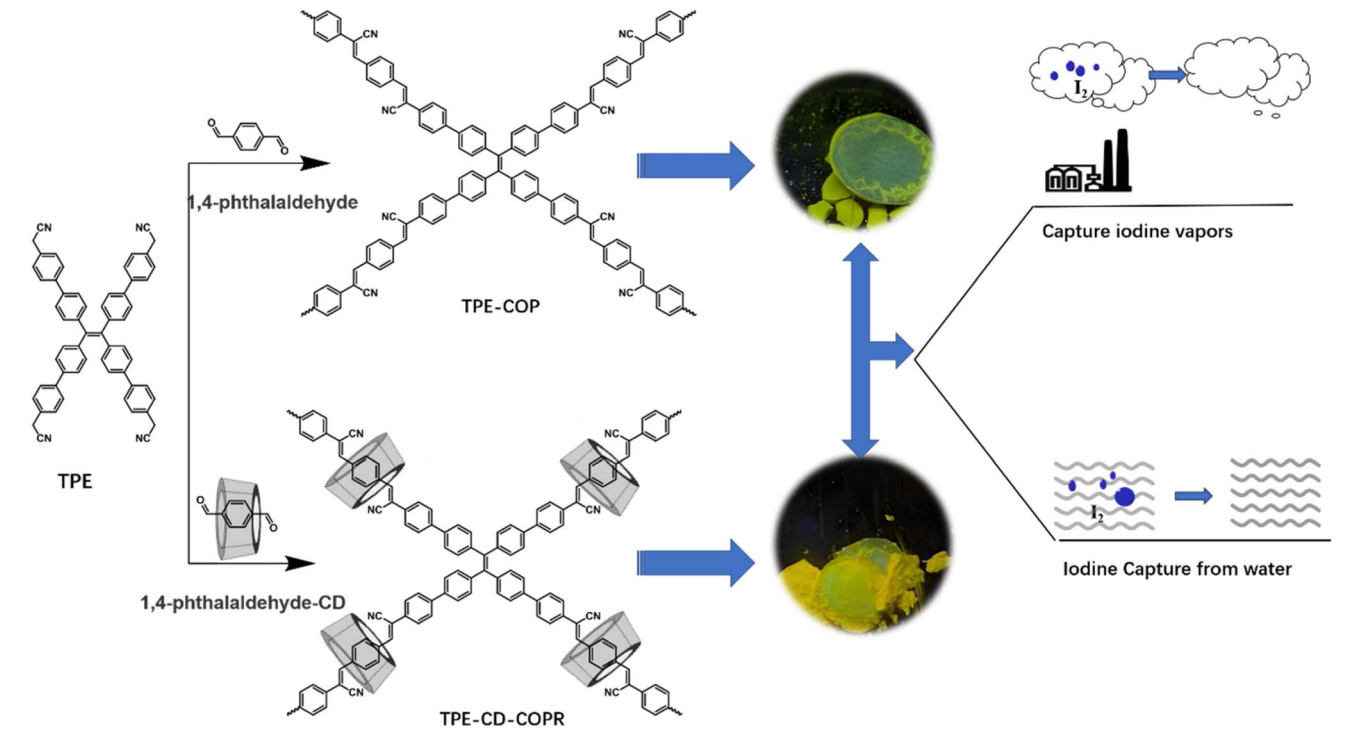

Scheme 1 Schematic route for the synthesis of cyanostilbene based TPE-COP and TPE-CD-COPR.

stoichiometric, base-catalyzed Knoevenagel condensation with 2,2′,2″,2‴-(ethene-1,1,2,2-tetrayltetrakis([1,1′-biphenyl]-4,4′-diyl))tetraacetonitrile (TPE). In a representative procedure, a tetrahydrofuran (THF) solution containing both aldehyde monomers and TPE was mixed with a methanol solution of Cs_2CO_3 catalyst. The reaction mixture was stirred at room temperature for 24 h under ambient atmosphere. The resulting precipitate was collected by vacuum filtration, which was successively washed with large amounts of water and methanol, and then subjected to rigorous purification *via* Soxhlet extraction with methanol (48 h) followed by acetone (24 h) to remove oligomeric species and unreacted monomers. The final solid material was dried under vacuum at 80 °C for 12 h, yielding solid-state luminescent materials, termed as TPE-COP (greenish-yellow solid-state emission) and TPE-CD-COPR (yellow solid-state emission).

The construction of the CD-threaded CS-network was unambiguously verified through complementary spectroscopic analyses *via* Fourier transform infrared spectroscopy (FT-IR) and solid-state ^{1}H–^{13}C CP/MAS NMR spectroscopy (solid state ^{13}C NMR), using the TPE-COP as control. Similar to the TPE-COP (Fig. S1a), the FT-IR spectrum of TPE-CD-COPR (Fig. 1a) also exhibited diagnostic vibrational bands of cyanostilbene units, including characteristic C=C stretching at 1590–1610 cm^{-1} and intense C≡N stretching at 2216–2219 cm^{-1}. However, apart from the feature peaks of TPE-COP, TPE-CD-COPR showed broad hydroxyl (–OH) stretching vibrations centered at 3410–3440 cm^{-1}.[23,24] Critically, the near-complete disappearance of the aldehyde C=O stretching band (1696–1700 cm^{-1}) indicated highly efficient polymerization conversion.[25]

Solid-state ^{13}C NMR spectroscopy further corroborated these structural insights, displaying well-resolved signals for both aliphatic and unsaturated carbon species for TPE-CD-COPR. In contrast to TPE-COP (Fig. S1b), the ^{13}C NMR spectrum of TPE-CD-COPR exhibits a broader distribution and higher density of carbon signals (Fig. 1b). A resonance near 20 ppm, attributable to CN groups, was observed in both samples, confirming the formation of the CS-based framework. For the TPE-CD-COPR, the upfield signals at 30.6 and 37.3 ppm are unambiguously assigned to sp^3-hybridized carbons within the cyclodextrin (CD) macrocycles.[26] On the other hand, the downfield resonances, observed at 104.7, 117.2, 129.5, 137.1, 151.2, 154.5, 164.2, and 173.8 ppm, correspond to aromatic structures in the covalent organic polyrotaxane.[27,28] Moreover, the absence of any signal in the δ = 190–200 ppm region confirms the complete consumption of aldehyde functional groups.[29] Together, these spectral characteristics offer compelling evidence for the successful polymerization and the threading of CD units within the resulting supramolecular architecture.

Thermogravimetric analysis (TGA, Fig. 1c) under N_2 revealed a well-defined multistage decomposition profile for the CD-threaded CS-network, providing unambiguous evidence of its hierarchical structural robustness. The material underwent

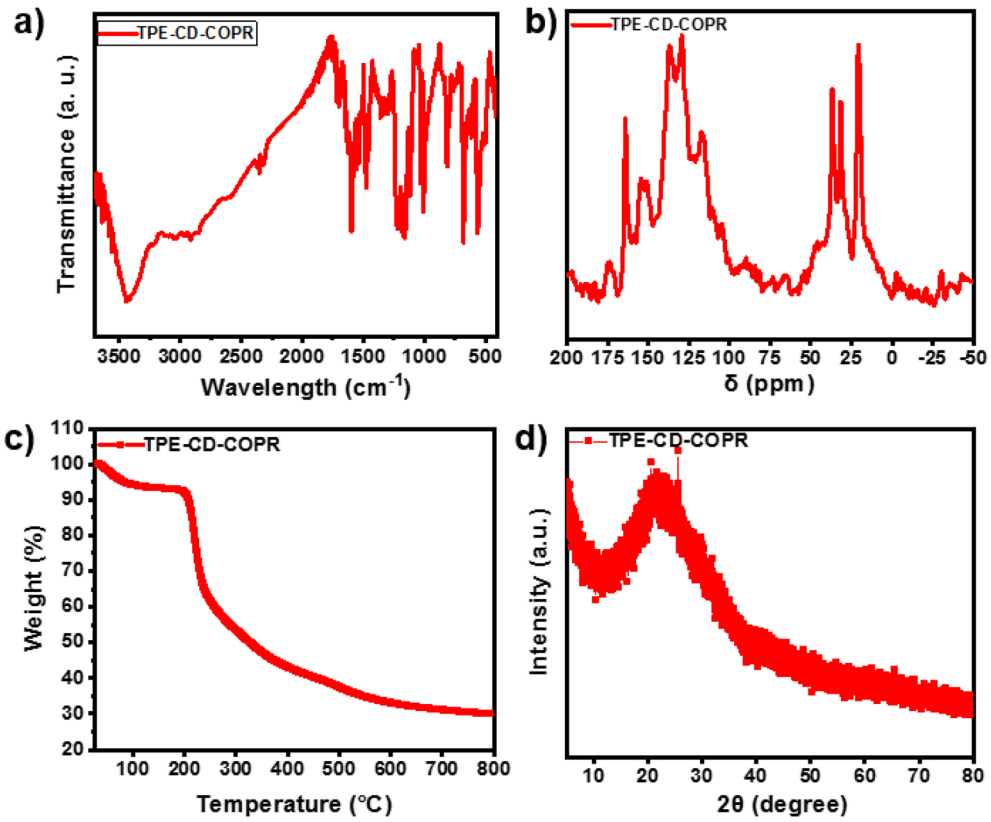

Fig. 1 Physical characterization of TPE-CD-COPR. (a) FT-IR of TPE-CD-COPR; (b) solid state ^{13}C NMR of TPE-CD-COPR; (c) TGA of TPE-CD-COPR; (d) XRD of TPE-CD-COPR.

three distinct thermal degradation stages, encompassing an initial dehydration (30–100 °C, 5.2% mass loss, attributed to adsorbed water evaporation), a framework decomposition (250–450 °C, 63.7% mass loss, corresponding to main-chain scission), and a carbonization plateau (>600 °C, residual mass >31%, indicating char formation). Notably, this stepwise degradation pathway exhibited significantly enhanced thermal stability relative to non-threaded analogs (which underwent complete decomposition below 280 °C, Fig. S1). Consistent with prior reports, supplementary power X-ray diffraction (XRD) analysis (Fig. 1d and S1d) further confirmed the amorphous nature of the synthesized materials, displaying only a broad diffraction peak at 26°, characteristic of noncrystalline covalent organic polymer.[29] The absence of crystalline peaks underscored the disordered cross-linking topology inherent to the threaded network structure.[30,31]

The properties and functions of materials are largely governed by their hierarchical architectures across multiple scales. To this end, the morphology of TPE-CD-COPR was investigated by transmission electron microscopy (TEM) and compared with that of TPE-COP (Fig. S2). At the micron scale (Fig. 2a and b), the TEM images reveal macro-stacking features, showing an assembly of quasi-layered particles that form a bicontinuous network of interconnected macropores and mesopores. At a higher resolution of 50 nm (Fig. 2c), the framework is shown to consist of nanosheets with lamellar stacking. Further nanoscale mapping (10 nm TEM/STEM, Fig. 2d) reveals a transition to amorphous stacking characteristics at the molecular level, alongside a homogeneous distribution of carbon, nitrogen, and oxygen across the nanosheet matrices. Similar case was detected for the TPE-COP, which was assembled by the 2D sheet like structure. Energy-dispersive X-ray spectroscopy (EDS) analysis (Fig. S3) quantified the elemental composition of TPE-CD-COPR as 47.8% C, 1.50% N, and 50.7% O, which contrasts markedly with the composition of TPE-COF (83.3% C, 4.34% N, 12.3% O). This significantly elevated oxygen content in TPE-CD-COPR provides strong evidence for the successful incorporation of

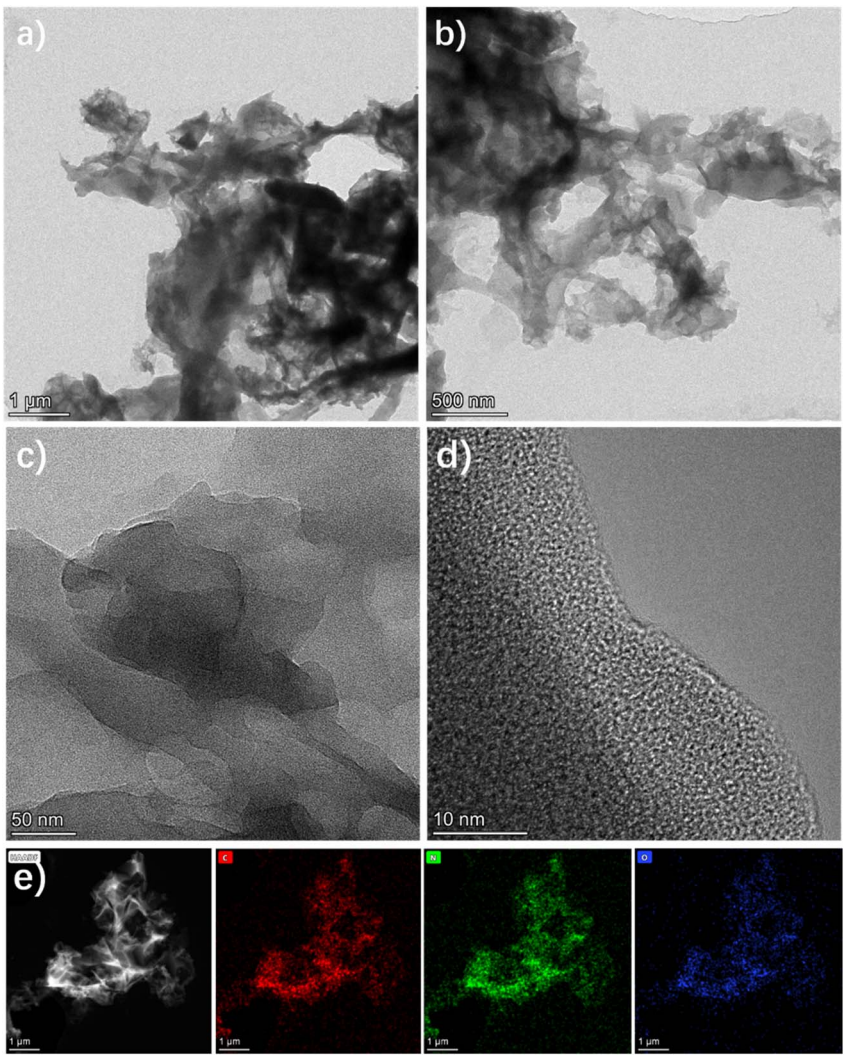

Fig. 2 TEM and corresponding HAADF elemental mapping of TPE-CD-COPR. (a–d) TEM of TPE-CD-COPR at varied scale bar of 1 μm, 500 nm, 50 nm and 10 nm, respectively. (e) Elemental mapping of TPE-CD-COPR at a scale bar of 1 μm.

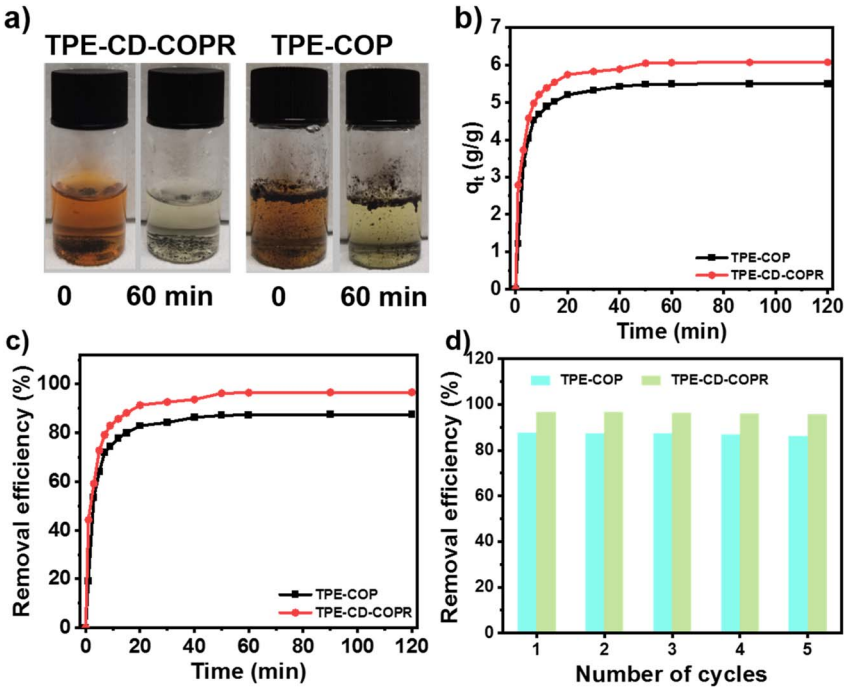

Fig. 3 Comparative analysis of iodine adsorption by TPE-COP and TPE-CD-COPR: (a) color change of aqueous iodine solutions before and after the addition of TPE-CD-COPR and TPE-COP for 60 min; (b) adsorption kinetics; (c) adsorption kinetics date for the TPE-CD-COPR and TPE-COP; (c) the removal efficiency for TPE-CD-COPR and TPE-COP; (d) reusability of TPE-COP and TPE-CD-COPR for 5 cycles.

cyclodextrin into the polyrotaxane structure facilitating iodine uptake.[32]

Then, the iodine adsorption capacity of TPE-CD-COPR from water was subsequently evaluated, using TPE-COP and pure β-CD as controls. All experiments were conducted under identical conditions (temperature, pressure, and initial concentration).[33] As clearly shown in Fig. 3a, TPE-CD-COPR demonstrated markedly improved water dispersibility compared to the cyclodextrin-free TPE-COP, a crucial enhancement that directly contributed to its superior adsorption performance. This improved dispersibility can be attributed to the incorporation of hydrophilic β-CD units.[34] Both TPE-COP (CD-free) and TPE-CD-COPR (CD-threaded) displayed rapid iodine uptake within the first 20 min, approaching equilibrium around 60 min (Fig. 3b). However, pure β-CD exhibited a significantly slower iodine capture rate in water, with 26% of iodine still remaining in the solution after 80 min (Fig. S4). During the adsorption process, a distinct visual change was observed that the initially dark brown iodine solution gradually lightened for all these samples. TPE-CD-COPR, in particular, showed more pronounced decolorization. This striking color transition correlated closely with the adsorption kinetic profile, providing clear visual evidence of the exceptional iodine capture ability of TPE-CD-COPR. As clearly illustrated in Fig. 3c, TPE-CD-COPR achieved nearly complete iodine removal (~100%) within 60 min, significantly outperforming TPE-COP (~87%).

The remarkable iodine adsorption performance of TPE-CD-COPR stems from multi-level synergistic effects among its three distinct structural components. The fully conjugated skeleton provides extended π-electron surfaces, while the nitrogen-rich heteroatomic sites enhance binding *via* lone-pair electron interactions. Concurrently, the threaded cyclodextrin (CD) units contribute O-bearing sites for effective iodine confinement. This integrated system, which synergizes the conjugated framework, nitrogen sites, and CDs, collectively enhances both adsorption capacity and affinity, ultimately establishing TPE-CD-COPR as a highly effective adsorbent for water purification.[35,36]

The adsorption isotherms of iodine onto the as-prepared samples were investigated by varying the initial iodine concentration at 25 °C. After treatment with the adsorbents (1.0 mg mL^{-1}), the residual iodine concentration was determined by UV-vis spectroscopy. The resulting data were fitted using both the Langmuir and Freundlich isotherm models (Fig. S2). The Freundlich model yielded higher linear correlation coefficients (R^2 = 0.976 for TPE-COP and 0.9914 for TPE-CD-COPR) than those obtained from the Langmuir model (R^2 = 0.952 and 0.961, respectively), indicating that the Freundlich model more accurately describes the adsorption process. These results suggest that iodine uptake occurs *via* multilayer adsorption on a heterogeneous surface, consistent with a synergistic adsorption mechanism involving multiple active sites.

The reusability of TPE-CD-COPR was assessed over five consecutive adsorption–desorption cycles (Fig. 3d). Remarkably, TPE-CD-COPR maintained ~99% of its initial adsorption capacity, whereas the reference material TPE-COP exhibited a discernible decrease to ~97%. This superior performance originates from the unique polyrotaxane framework, in which the mechanically interlocked β-CD units contribute exceptional

structural integrity, effectively preventing pore collapse, enhancing resistance to bond dissociation, and creating an innovative molecular-scale shielding effect. The cyclodextrin components play a dual protective role: they help preserve pore accessibility while simultaneously safeguarding active sites. These attributes collectively underscore the competitive adsorption capacity and outstanding reusability of TPE-CD-COPR, comparable to or surpassing that of other porous polymers and cyclodextrin-based adsorbents summarized in Table S1. Such synergistic properties position TPE-CD-COPR as a promising benchmark for the development of highly stable and reusable adsorbents in water treatment applications.

Iodine vapor uptake by TPE-CD-COPR and TPE-COP was monitored under identical conditions. Both sorbents captured more than seventy percent of their final capacity within 10 h, yet TPE-CD-COPR proceeded 23% faster than TPE-COP. The adsorption reached equilibrium after 30 h, revealing a remarkable 30.8% higher capacity for TPE-CD-COPR (0.85 *vs.* 0.65 g g^{-1}). The higher performance of TPE-CD-COPR rests on the effects of CD threading. The polyrotaxane-embedded β-CD opens more active sites, accelerating early uptake. Extra binding pockets created by CD enlarge the saturation level. Together these factors give TPE-CD-COPR a decisive edge in iodine capture. The unique polyrotaxane architecture creates a molecular environment that simultaneously enhances critical performance aspects with binding site accessibility for faster kinetics, and increased iodine accommodation capacity. This multi-level enhancement mechanism fully explains the consistent performance advantage observed throughout the entire adsorption profile, making TPE-CD-COPR a superior iodine capture material.

Conclusion

This study demonstrates that the strategic incorporation of cyclodextrin (CD) into conjugated porous polyrotaxanes (CPPT) offers a versatile approach to simultaneously enhance solid-state luminescence and iodine adsorption performance. By threading β-cyclodextrin into the polymer skeleton, the resulting materials exhibit tunable aggregation-induced emission (AIE) properties, enabling precise control over emission color and intensity. More importantly, the CD-based polyrotaxane architecture significantly improves iodine capture efficiency, achieving near-complete removal (∼100%) from aqueous solutions and a 30.8% increase in vapor-phase adsorption capacity compared to non-threaded counterparts. The enhanced performance stems from synergistic effects, including optimized pore confinement, enriched oxygen-containing binding sites, and robust host–guest interactions. Furthermore, the mechanically interlocked structure ensures exceptional stability and reusability, retaining ∼99% efficiency after multiple cycles. This work highlights cyclodextrin threading as a powerful strategy to engineer multifunctional porous materials with tailored optoelectronic and environmental remediation capabilities, paving the way for advanced applications in solid-state lighting, iodine capture, and antimicrobial materials.

Conflicts of interest

There are no conflicts to declare.

Data availability

Data will be made available on request.

Supplementary information is available. See DOI: **https://doi.org/10.1039/d5ra06071k**.

References

1 Z. Xiang, D. Cao and L. Dai, *Polym. Chem.*, 2015, **6**, 1896–1911.
2 Q. Cheng, M. Wang, S. Liu, L. Zhang, H. Ji, Y. He, N. Li, T. Qian, C. Yan and J. Lu, *Angew. Chem., Int. Ed.*, 2023, **62**, e202308262.
3 Q. Yue, X. Wang, Y. Liu, D. Xu, Y. Ma, J. Wang, W. Bian and B. Zhou, *Chem. Eng. J.*, 2025, **517**, 164311.
4 Y. Ma, Q. Liu, F. Zhang, H. Xu, A. Zheng, X. Sun, J. Zhang, B. Wang, J. Hao and B. Zhou, *ACS Appl. Polym. Mater.*, 2025, **7**, 8457–8470.
5 Y. Wang, J. Wang, X. Ding, X. Yu, Y. Zhao, Z. Pan, L. Xu, W. Cheng, M. Ji, C. Yuan, T. Wang and B. Zhou, *ACS Appl. Polym. Mater.*, 2024, **6**, 13764–13774.
6 Z. Xiang, X. Zhou, C. Zhou, S. Zhong, X. He, C. Qin and D. Cao, *J. Mater. Chem.*, 2012, **22**, 22663–22669.
7 T. Skorjanc, D. Shetty and A. Trabolsi, *Chem*, 2021, **7**, 882–918.
8 M. Xue, L. Zhang, X. X. Li, Z. Chen, F. Kang, X. Wang, Q. Dong, X. Wang, C. Lee, Y. Lan and Q. Zhang, *Nat. Commun.*, 2024, **15**, 10026.
9 H. Zhu, Y. Qin, Y. Guo, Z. Shen, M. Imran, M. A. Mushtaq, Z. Zhang, C. Ni, Y. Chen, Y. Ding, H. Gul, J. Zou, P. Tsiakaras, H.-Y. Hsu and J. Zhao, *Chem. Eng. J.*, 2024, **484**, 149739.
10 C.-A. Wang, Y.-W. Li, Y.-F. Han, J.-P. Zhang, R.-T. Wu and G.-F. He, *Polym. Chem.*, 2017, **8**, 5561–5569.
11 D. Rodríguez-San-Miguel, C. Montoro and F. Zamora, *Chem. Soc. Rev.*, 2020, **49**, 2291–2302.
12 N. Enjamuri, S. Sarkar, B. M. Reddy and J. Mondal, *Chem. Rec.*, 2019, **19**, 1782–1792.
13 T. Guo, Y. Wang, J. Li, X. Ding, Q. Sun, J. Yuan, L. Ma, H. Hao and B. Zhou, *ACS Appl. Nano Mater.*, 2024, **7**, 17391–17405.
14 C. Miao, L. Chu, D. Guo, X. Ding, W. Guo, S. Wang, J. Sheng, J. Zhang, Z. Wang and B. Zhou, *J. Environ. Chem. Eng.*, 2023, **11**, 110514.
15 C. Miao, N. Tang, L. Shi, S. Wang, P. Ji, J. Zhang, Z. Wang and B. Zhou, *ACS Appl. Polym. Mater.*, 2023, **5**, 8679–8692.
16 W. Xie, D. Cui, S.-R. Zhang, Y.-H. Xu and D.-L. Jiang, *Mater. Horiz.*, 2019, **6**, 1571–1595.
17 A. M. Musuc, *Molecules*, 2024, **29**, 5319.
18 M. Á. Esteso and C. M. Romero, *Int. J. Mol. Sci.*, 2024, **25**, 4547.
19 Y. Li, F. Liu, T. Abdiryim and X. Liu, *Coord. Chem. Rev.*, 2024, **502**, 215613.
20 Z. Li and Y. Yang, *Adv. Mater.*, 2022, **34**, 2107401.

21 W. Chen, P. Chen, G. Zhang, G. Xing, Y. Feng, Y. Yang and L. Chen, *Chem. Soc. Rev.*, 2021, **50**, 11684–11714.
22 X. Guo, J. Yu, L. Ma, J. Yuan, T. Guo, Y. Ma, S. Xiao, J. Bai and B. Zhou, *RSC Adv.*, 2024, **14**, 30077–30083.
23 Y. Wei, W. Chen, X. Zhao, S. Ding, S. Han and L. Chen, *Polym. Chem.*, 2016, **7**, 3983–3988.
24 C. Yuan, B. Liu and H. Liu, *Carbohydr. Polym.*, 2015, **118**, 36–40.
25 C. Tengroth, U. Gasslander, F. O. Andersson and S. P. Jacobsson, *Pharm. Dev. Technol.*, 2005, **10**, 405–412.
26 C. Yuan, X. Wu, R. Gao, X. Han, Y. Liu, Y. Long and Y. Cui, *J. Am. Chem. Soc.*, 2019, **141**, 20187–20197.
27 S. Li, O. Lafon, W. Wang, Q. Wang, X. Wang, Y. Li, J. Xu and F. Deng, *Adv. Mater.*, 2020, **32**, 2002879.
28 Y. Hou, P. Zhou, F. Liu, Y. Lu, H. Tan, Z. Li, M. Tong and J. Ni, *Angew. Chem., Int. Ed.*, 2024, **63**, e202318562.
29 Y. Sang, Y. Cao, L. Wang, W. Yan, T. Chen, J. Huang and Y.-N. Liu, *J. Colloid Interface Sci.*, 2021, **587**, 121–130.
30 B. Zhou, L. Liu, Z. Yang, X. Li, Z. Wen and L. Chen, *ChemElectroChem*, 2019, **6**, 485–492.
31 B. Zhou, F. Yan, X. Li, J. Zhou and W. Zhang, *ChemSusChem*, 2019, **12**, 915–923.
32 J. Yuan, J. Yu, L. Ma, Y. Ma, H. Hao, C. Zhao and B. Zhou, *J. Environ. Chem. Eng.*, 2024, **12**, 114531.
33 C. Wang, Y. Wang, R. Ge, X. Song, X. Xing, Q. Jiang, H. Lu, C. Hao, X. Guo, Y. Gao and D. Jiang, *Chem.–Eur. J.*, 2018, **24**, 585–589.
34 J. Li, J. Yuan, G. Sun, W. Li, H. Hao and B. Zhou, *RSC Adv.*, 2024, **14**, 30364–30377.
35 J. Chen, T. Guo, X. Ren, T. Yang, K. Zhang, Y. Guo, X. Chen, S. Gui, S. Wang, Q. Li, C. Peng, J. Zhang and L. Wu, *Carbohydr. Polym.*, 2022, **291**, 119507.
36 Y. Cai, J. Li, Q. Zhang, C. Liu, C. Wang, H. Shi, L. Jiang and D. Wu, *Sep. Purif. Technol.*, 2025, **376**, 134078.